areas of downwelling across the 660 is consistent with the occurrence of dehydration melting as observed in our laboratory experiments. An alternative bulk-compositional origin of low velocities near the top of the lower mantle is segregated basalt that may be neutrally buoyant (*23*) and would reduce seismic velocities (*24*).

However, long-term accumulation of basalt near the top of the lower mantle is not expected to be preferentially present where there is downwelling across the 660 and absent where there is not. The areas of downward flow across 660 do not all coincide with local presence of subducted slabs, so a direct link to composition of the sinking Farallon slab cannot explain the negative velocity gradients below 660. Assuming that the velocity reductions result from partial melt, and that the shear-velocity decrease per percent of melt is between 2.6 and 3.8%, as predicted for partial melt near 400-km depth (*25*), then 0.68 to 1% melt could explain a 2.6% shear velocity reduction indicated by negative *Ps* conversions with amplitude of 2% in the CCP image.

Prediction of partial melt percentages at 660-km depth for various H_2O contents requires knowledge of water partition coefficients between minerals and melts at relevant pressure-temperature (*P-T*) conditions in the peridotite-saturated compositional system. At present, experiments in the hydrous peridotite system at conditions near the 660 have not been performed. However, using experimental results for partial melting near the 410-km discontinuity (410) in a bulk peridotite system with 1 wt % H_2O indicates that ~5% partial melt at 410 km is expected (*26*, *27*) where the partition coefficient of H_2O between wadsleyite and olivine is at least 5:1 (*11*). We can expect at least 5% partial melt in a bulk 1 wt % H_2O peridotite system where the partition coefficient between ringwoodite and silicate perovskite is 15:1 (*11*). Thus, production of up to 1% melt by dehydration melting of hydrous ringwoodite viscously entrained into the lower mantle is feasible.

The density of hydrous melt near the top of the lower mantle is uncertain, but it is likely buoyant with respect to the top of the lower mantle (*28*). Hence, we expect that the velocity decreases imaged beneath the 660 are transient features resulting from ongoing downward flow through the 660 that is driven by sinking slabs in the lower mantle. Eventually, the slightly buoyant hydrous melt would percolate upward, returning H_2O to the transition zone (*4*). Dehydration melting has also been suggested to occur where hydrous wadsleyite upwells across the 410 and into the olivine stability field (*3*, *27*). Experiments indicate that hydrous melt is gravitationally stable atop the 410 (*28*), so once melt is generated, it may remain or spread laterally rather than maintaining a clear correlation with ongoing vertical flow patterns. Seismic detections of a low-velocity layer atop the 410 are common but laterally sporadic beneath North America and globally (*29*, *30*). The combination of dehydration melting driven by downwelling across the 660 and upwelling across the 410 could create a long-term H_2O trap in the transition zone (*4*).

REFERENCES AND NOTES

1. A. E. Saal, E. H. Hauri, C. H. Langmuir, M. R. Perfit, *Nature* **419**, 451–455 (2002).
2. J. R. Smyth, *Am. Mineral.* **72**, 1051 (1987).
3. D. L. Kohlstedt, H. Keppler, D. C. Rubie, *Contrib. Mineral. Petrol.* **123**, 345–357 (1996).
4. D. Bercovici, S. Karato, *Nature* **425**, 39–44 (2003).
5. D. G. Pearson *et al.*, *Nature* **507**, 221–224 (2014).
6. H. Zhu, E. Bozdag, T. S. Duffy, J. Tromp, *Earth Planet. Sci. Lett.* **381**, 1–11 (2013).
7. A. Kelbert, A. Schultz, G. Egbert, *Nature* **460**, 1003–1006 (2009).
8. N. Bolfan-Casanova, H. Keppler, D. C. Rubie, *Geophys. Res. Lett.* **30**, 1905 (2003).
9. M. Murakami, K. Hirose, H. Yurimoto, S. Nakashima, N. Takafuji, *Science* **295**, 1885–1887 (2002).
10. K. Litasov *et al.*, *Earth Planet. Sci. Lett.* **211**, 189–203 (2003).
11. T. Inoue, T. Wada, R. Sasaki, H. Yurimoto, *Phys. Earth Planet. Inter.* **183**, 245–251 (2010).
12. Materials and methods are available on *Science* Online.
13. S. D. Jacobsen, J. R. Smyth, H. A. Spetzler, C. M. Holl, D. J. Frost, *Phys. Earth Planet. Inter.* **143-144**, 47–56 (2004).
14. R. A. Kerr, *Science* **340**, 1283–1285 (2013).
15. J. P. Mercier, M. G. Bostock, A. M. Baig, *Geophysics* **71**, SI95–SI102 (2006).
16. B. Schmandt, K. G. Dueker, E. D. Humphreys, S. M. Hansen, *Earth Planet. Sci. Lett.* **331-332**, 224–236 (2012).
17. B. Tauzin, R. D. van der Hilst, G. Wittlinger, Y. Ricard, *J. Geophys. Res. Solid Earth* **118**, 2307–2322 (2013).
18. J. Ritsema, A. Deuss, H. J. van Heijst, J. H. Woodhouse, *Geophys. J. Int.* **184**, 1223–1236 (2011).
19. T. W. Becker, C. Faccenna, E. D. Humphreys, A. R. Lowry, M. S. Miller, *Earth Planet. Sci. Lett.* (2014).
20. N. A. Simmons, A. M. Forte, S. P. Grand, *Geophys. J. Int.* **177**, 1284–1304 (2009).
21. B. Steinberger, *Phys. Earth Planet. Inter.* **118**, 241–257 (2000).
22. A. M. Forte, R. Moucha, N. A. Simmons, S. P. Grand, J. X. Mitrovica, *Tectonophysics* **481**, 3–15 (2010).
23. C. T. A. Lee, W. P. Chen, *Earth Planet. Sci. Lett.* **255**, 357–366 (2007).
24. W. B. Xu, C. Lithgow-Bertelloni, L. Stixrude, J. Ritsema, *Earth Planet. Sci. Lett.* **275**, 70–79 (2008).
25. S. Hier-Majumder, A. Courtier, *Earth Planet. Sci. Lett.* **308**, 334–342 (2011).
26. M. M. Hirschmann, T. Tenner, C. Aubaud, A. C. Withers, *Phys. Earth Planet. Inter.* **176**, 54–68 (2009).
27. T. J. Tenner, M. M. Hirschmann, A. C. Withers, P. Ardia, *Contrib. Mineral. Petrol.* **163**, 297–316 (2012).
28. T. Sakamaki, A. Suzuki, E. Ohtani, *Nature* **439**, 192–194 (2006).
29. B. Schmandt, K. G. Dueker, S. M. Hansen, J. J. Jasbinsek, Z. Zhang, *Geochem. Geophys. Geosyst.* **12**, Q08014 (2011).
30. B. Tauzin, E. Debayle, G. Wittlinger, *Nat. Geosci.* **3**, 718–721 (2010).

ACKNOWLEDGMENTS

Seismic data were acquired from the IRIS Data Management Center. This work was supported by NSF grants EAR-0748707 to S.D.J. and EAR-1215720 to T.W.B., and by the David and Lucile Packard Foundation and Carnegie/DOE Alliance Center (CDAC) to S.D.J. Portions of this work were performed at GSECARS (Sector 13), Advanced Photon Source (APS), Argonne National Laboratory. GSECARS is supported by the NSF (EAR-1128799) and U.S. Department of Energy (DOE) (DE-FG02-94ER14466). Use of the APS was supported by the DOE-BES (Basic Energy Sciences) (DE-AC02-06CH11357). Portions of this work were performed at beamline U2A of the National Synchrotron Light Source (NSLS), Brookhaven National Laboratory. U2A is supported by COMPRES (Consortium for Materials Properties Research in Earth Sciences) under NSF Cooperative Agreement EAR 11-57758 and DOE-NNSA (National Nuclear Security Administration) (DE-FC-52-08NA28554, CDAC). Use of the NSLS was supported by the DOE-BES (DE-AC02-98CH10886). We thank S. Demouchy, D. J. Frost, E. H. Hauri, M. M. Hirschmann, F. Langenhorst, J. F. Lin, G. Shen, V. B. Prakapenka, and J. R. Smyth for discussions and help with experiments. B.S. and S.D.J. designed the research and wrote the paper. B.S. conducted the seismological research, and S.D.J. performed the experiments. T.W.B. produced the mantle circulation models, Z.L. contributed to the FTIR experiments, and K.G.D. contributed to seismic imaging. All authors participated in data interpretation and contributed to the manuscript.

SUPPLEMENTARY MATERIALS

www.sciencemag.org/content/344/6189/1265/suppl/DC1
Materials and Methods
Figs. S1 to S4
References (*31*–*38*)
Additional Data Tables S1 to S3

13 March 2014; accepted 12 May 2014
10.1126/science.1253358

DINOSAUR PHYSIOLOGY

Evidence for mesothermy in dinosaurs

John M. Grady,[1]* Brian J. Enquist,[2,3] Eva Dettweiler-Robinson,[1] Natalie A. Wright,[1] Felisa A. Smith[1]

Were dinosaurs ectotherms or fast-metabolizing endotherms whose activities were unconstrained by temperature? To date, some of the strongest evidence for endothermy comes from the rapid growth rates derived from the analysis of fossil bones. However, these studies are constrained by a lack of comparative data and an appropriate energetic framework. Here we compile data on ontogenetic growth for extant and fossil vertebrates, including all major dinosaur clades. Using a metabolic scaling approach, we find that growth and metabolic rates follow theoretical predictions across clades, although some groups deviate. Moreover, when the effects of size and temperature are considered, dinosaur metabolic rates were intermediate to those of endotherms and ectotherms and closest to those of extant mesotherms. Our results suggest that the modern dichotomy of endothermic versus ectothermic is overly simplistic.

Over the past few decades, the original characterization of dinosaurs by early paleontologists as lumbering, slow-metabolizing ectotherms has been challenged. Recent studies propose that dinosaurs were capable of an active lifestyle and were metabolically similar to endothermic mammals and birds (*1*–*3*). This debate is of more than heuristic interest; energy consumption is closely linked to life history, demographic, and ecological traits (*4*). Extant endothermic mammals and birds possess metabolic rates ~5 to 10 times higher than

Downloaded from http://science.sciencemag.org/ on July 5, 2016

those of reptiles and fish (*5*, *6*), but characterizing the metabolic rates of dinosaurs has been difficult.

A promising method for inferring paleoenergetics comes from studies of ontogenetic growth, in which age is determined from annual rings in bone cross sections and mass is determined from bone dimensions. Ultimately, growth is powered by metabolism, and rates of growth and energy use should correspond. Pioneering work by Erickson and others has led to a growing body of literature on dinosaur growth and generated important insights (*7*, *8*). However, many analyses were hampered by small samples, an outdated comparative data set, and the lack of an appropriate energetic framework. Increasing data availability permits a reassessment of dinosaur growth against a broader spectrum of animals, standardized for environmental temperature. Further, recent advances in metabolic theory provide a theoretical framework for evaluating metabolic rate on the basis of growth.

We used a comparative approach to characterize the energetics of dinosaurs and other extinct taxa. We examined the empirical and theoretical relationship between growth and resting metabolic rate, using a broad database of major vertebrate clades (*9*), and used our results to examine the energetics of Mesozoic dinosaurs. From empirical studies, we constructed ontogenetic growth curves and determined a maximum rate of growth for each species. Environmental temperature was standardized by only considering growth rates in ectotherms from tropical and subtropical climates or from laboratory settings between 24° and 30°C, comparable to temperatures experienced by dinosaurs during the Mesozoic (*10*). Data for dinosaur growth were taken from published reports that provided a minimum of five measurements of size and age. All metabolic rates were converted to watts (W). Where multiple metabolic or maximum growth rates for a species were recorded, the geometric mean was determined. Overall, our data set includes ~30,000 values and was used to characterize growth for 381 species, including 21 species of Mesozoic dinosaurs, 6 extinct crocodilians, and a Cretaceous shark (table S1). Dinosaurs are well represented both temporally (late Triassic to end-Cretaceous) and taxonomically (Theropoda, Sauropodomorpha, Ornithopoda, and Ceratopsia). Values for resting metabolic rates were compiled from the literature and standardized to a common temperature of 27°C (table S1). We performed phylogenetic independent contrasts (PICs) in addition to conventional ordinary least-squares regression (OLS) and standardized major axis regression (table S2).

Data show, within and across species, that resting metabolic rate B scales with body mass m as a power function, $B = B_0 m^{\alpha}$, where B_0 is

[1]Department of Biology, University of New Mexico, Albuquerque, NM 87131, USA. [2]Department of Ecology and Evolutionary Biology, University of Arizona, Tucson, AZ 85721, USA. [3]The Santa Fe Institute, USA, 1399 Hyde Park Road, Santa Fe, NM 87501, USA.
*Corresponding author. E-mail: jgrady@unm.edu

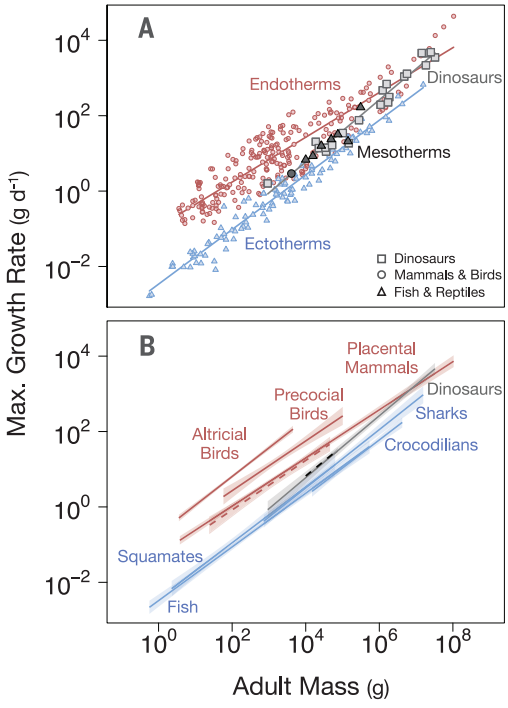


Fig. 1. The scaling of maximum growth rate in vertebrates. (**A**) Growth rates of thermoregulatory guilds. Red indicates endothermy; blue, ectothermy, gray, dinosaurs; and black, mesothermy. (**B**) Vertebrate taxa scaling with 95% confidence bands. The red dashed line indicates marsupials, and the black dashed line is tuna; all other taxa are labeled. See table S2 for regression parameters and statistics.

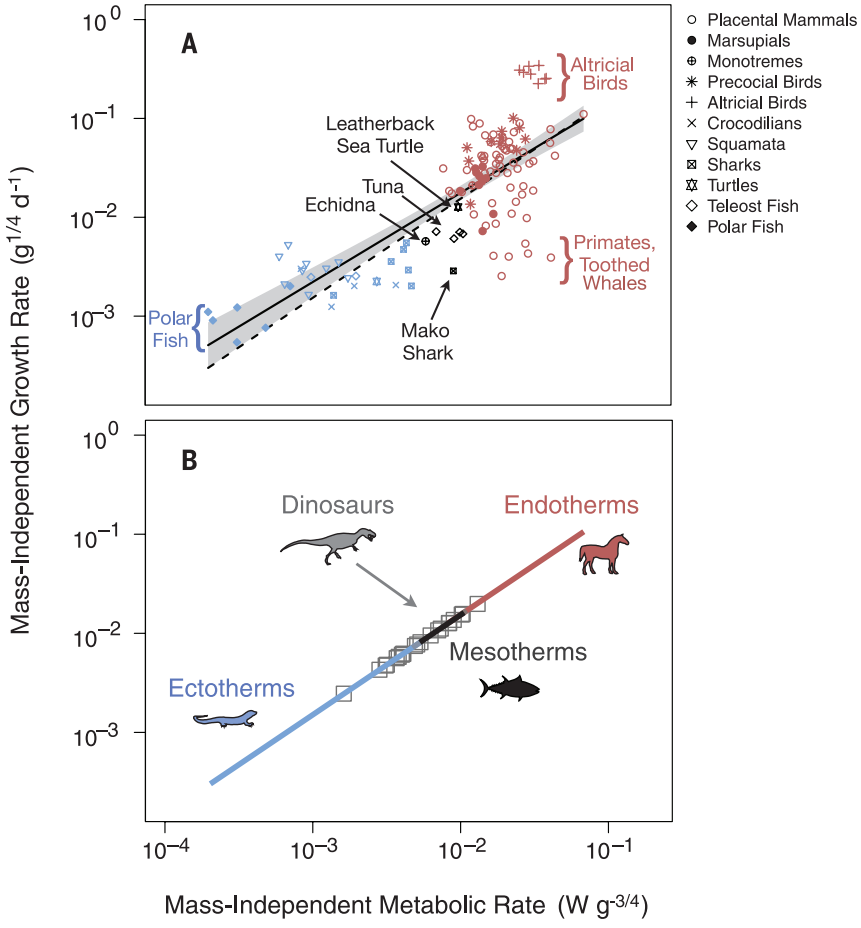


Fig. 2. Vertebrate growth energetics. (**A**) Relationship between growth and resting metabolic rate for vertebrates. The dashed line is the theoretical prediction; the solid line represents an OLS fitted regression with 95% confidence bands. (**B**) Predicted energetics of dinosaurs. Dinosaur rates (open squares) from Eq. 2 are plotted on the theoretical line. The ranges in metabolic rates occupied by extant endotherms, mesotherms, and ectotherms are indicated by color.

Downloaded from http://science.sciencemag.org/ on July 5, 2016

a normalization constant representing mass-independent metabolic rate, and α is ~3/4 and ranges from 0.65 to 0.85 (*11*, *12*). Growth rate varies over ontogeny, but use of the maximum growth rate (G_{max}) standardizes growth and permits interspecific comparisons. Empirical evidence (*13*) indicates that G_{max} scales similarly to B, where $G_{max} = G_0 M^{\alpha}$. This suggests that $B \propto G_{max}^{1}$ and thus that metabolic rate may be inferred from growth. However, the relationship between G_{max} and B across major vertebrate taxa has received little attention, and many uncertainties exist. For instance, Case (*13*) reported that fish G_{max} was an order of magnitude lower than that of reptiles, despite similarities in metabolic and thermoregulatory lifestyle (*6*).

Theoretical assessments of growth complement a strictly empirical approach and can strengthen paleontological inferences. An ontogenetic growth model based on metabolic scaling theory (MST) quantifies the linkages between G_{max} and metabolic rate from first principles of allometry and conservation of energy (*14*, *15*). According to MST (*9*), the relationship between B (W) and G_{max} (g day^{-1}) at final adult mass M is

$$B_M = cG_{max}^{1} \quad (1)$$

where $c \approx 0.66$ (W g^{-1} day). To observe the mass-independent relationship and compare energetic groups, we divide both sides by M^{α}, yielding

$$B_0 = cG_0 \quad (2)$$

To calculate metabolic rate at any ontogenetic mass m from the observed maximum growth rate, we combine Eqs. 1 and 2

$$B_m = cG_0 m^{3/4} \quad (3)$$

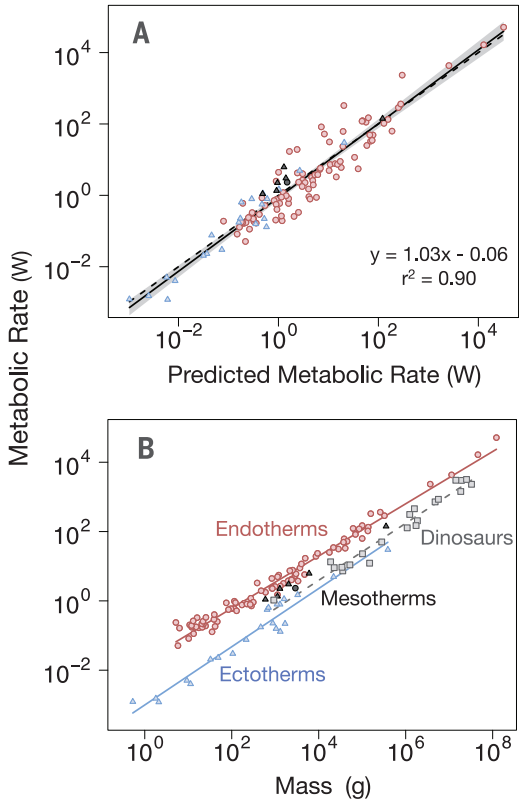


Fig. 3. Resting metabolic rates in vertebrates. (**A**) Predicted metabolic rates compared to observed rates. The solid line is the fitted regression, with shaded 95% confidence bands; the dashed line is the theoretical fit. (**B**) Metabolic scaling of vertebrates. Dinosaur resting metabolic rates are predicted from growth (dashed line); all other fits are predicted from empirical data. Endotherms: $y = 0.019x^{0.75}$, $r^2 = 0.98$, $n = 89$; Ectotherms (27°C): $y = 0.00099x^{0.84}$, $r^2 = 0.95$, $n = 22$; Dinosaurs: $y = 0.0020x^{0.82}$, $r^2 = 0.96$, $n = 21$. $P < 0.001$ for all regressions.

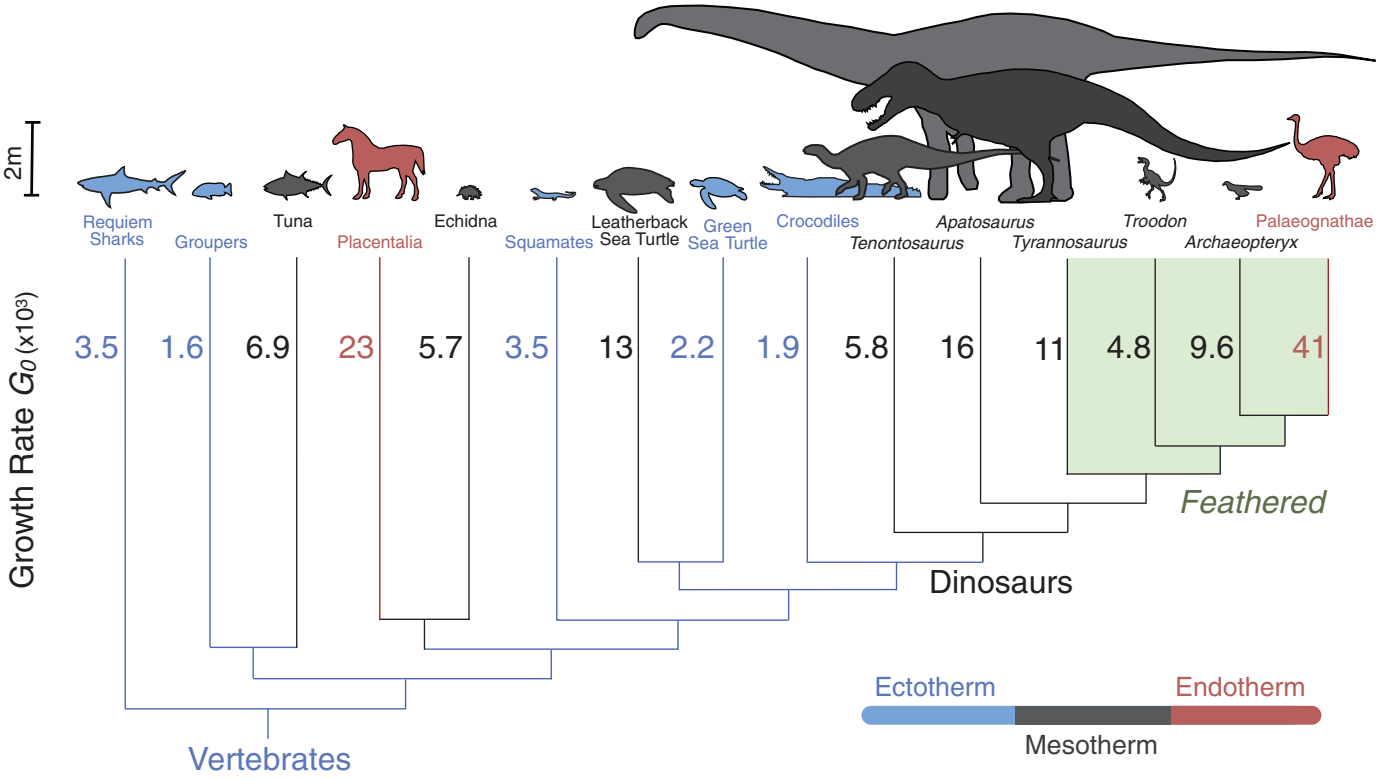


Fig. 4. Phylogeny of mass-independent growth rates (g$^{1/4}$ day^{-1}). Color signifies thermoregulatory state; branch lengths are not standardized for divergence times. Green shading indicates feathered coelurosaurian dinosaurs.

Downloaded from http://science.sciencemag.org/ on July 5, 2016

MST makes the following theoretical predictions regarding growth and metabolic rate:

(1) G_{max} scales as M^{α}, where $\alpha \sim 3/4$.

(2) B scales isometrically with G_{max} if masses are standardized (*9*). Regression of B against G_{max} yields a slope of 1 and an intercept of ≈0.66.

(3) Plotting G_0 against B_0 will reveal distinct energetic clusters corresponding to endotherms and ectotherms. High-power endotherms will exhibit an elevated G_0 and B_0, and ectothermic organisms the converse. Thermally intermediate taxa, termed mesotherms, such as tuna and lamnid sharks (*16*), should fall between the upper and lower quadrats. The predicted slope and intercept are 1 and 1.52, respectively. Similar clustering is observed if G_{max} and B residuals are plotted.

(4) $B_{predicted} = B_{observed}$ in extant animals, where $B_{predicted}$ is calculated from Eq. 3.

Our analyses find broad support for all four predictions. First, growth scales with mass as ~3/4, although taxonomic variation is observed (Fig. 1 and fig. S1, mean $\alpha_{OLS} = 0.73$; mean $\alpha_{PIC} = 0.69$, table S2). This indicates that larger species acquire their bulk by accelerating their maximum growth rate proportionate to $\sim M^{3/4}$. Second, G_{max} is a strong predictor of B, where $B_M = 0.56 G_{max}^{1.03}$, which is close to theoretical predictions [figs. S3 and S4; slope confidence interval (CI) = 0.97 to 1.10; intercept CI = 0.47 to 0.97; coefficient of determination (r^2) = 0.90, n = 118]. Third, we find that the observed relationship between mass-independent growth and metabolic rates corresponds closely to predicted values (slope = 0.90, CI = 0.77 to 1.03; intercept = 1.10, CI = 0.59 to 2.06, r^2 = 0.61, n = 124). Ectothermic species fall in the lower left quadrat; endotherms in the upper right; and thermally intermediate taxa, including tuna, a lamnid shark, the leatherback turtle, and a prototherian mammal, fall between values for endo- and ectotherms (Fig. 2 and figs. S1, S2, and S5). These results are robust; the inclusion of cold-water fish, with reduced growth and metabolic rates, simply extends the lower portion of the regression line. Furthermore, the ratio G_0/B_0 (g J^{-1}), a measure of efficiency in converting energy to biomass, does not differ significantly between endo- and ectotherms, indicating that energy allocation to growth does not vary with thermoregulatory strategy (t statistic = 0.46, P = 0.64, fig. S6). Finally, regression of observed against calculated metabolic rates does not differ significantly from unity (Fig. 3A; slope CI = 0.97 to 1.10; intercept CI = −0.14 to 0.02). We can therefore predict dinosaur resting metabolic rates from growth rate, using either a theoretical model (Eq. 3) or an empirically determined equation (*9*)

$$B_M = 0.6\, G_{max} \quad (4)$$

Our analyses are robust to variation in the scaling exponent, phylogenetic correction, inclusion of captive versus wild animals, critiques of dinosaur growth studies, and uncertainty in estimating M and metabolic temperature (*9*).

Our results find that mass-independent growth rates in dinosaurs were intermediate to, and significantly different from, those of endothermic and ectothermic taxa (table S2). Although some dinosaur growth rates overlap with high-power ectotherms or low-power endotherms, they cluster closest to energetically and thermally intermediate taxa, such as tuna (Fig. 2). Further, our analyses uphold the somewhat surprising finding that feathered dinosaurs, including protoavian *Archaeopteryx* (*17*), did not grow markedly differently from other dinosaurs (Fig. 4). It appears that modern avian energetics did not coincide with feathers or flight, which is consistent with fossil evidence that modern bone histology in birds did not appear until the late Cretaceous (*18*).

At the largest body masses, the growth rates of the largest dinosaurs and mammals overlap (Fig. 1B). This pattern is driven by two factors. First, dinosaurs have a relatively high slope (α_{OLS} = 0.82, but α_{PIC} = 0.76). This value is consistent with suggestions of thermal inertia for larger taxa; the removal of sauropods yields a reduced OLS slope of 0.77. Second, significantly reduced growth rates are observed in several large mammalian taxa, particularly primates, elephants, and toothed whales, whereas small shrews and rodents have relatively high rates, leading to a low overall slope for placental mammals (α_{OLS} = 0.64, α_{PIC} = 0.63; table S2 and fig. S11). The slow growth of many large endothermic mammals is associated with large brain size and low juvenile mortality (*19*, *20*); this is unlikely to be relevant to most dinosaurs.

Our results highlight important similarities and differences from previous studies. For example, our work agrees with assessments by Erickson (*7*, *17*) that dinosaurs grew at rates intermediate to most endo- and ectotherms. However, we find considerably more similarity in ectothermic growth rates than reported by Case (*13*) and significantly higher growth rates for fish (~seven times higher), marsupials (~four times higher) and precocial birds (~two times higher; fig. S8). We attribute these differences to enhanced sampling and standardization of the thermal environment for ectotherms (e.g., Case included temperate fish). Moreover, our expansion of the comparative growth framework indicates that dinosaurs grew and metabolized at rates most similar to those of active sharks and tuna (Fig. 2 and fig. S1), rather than those of endothermic marsupials, as has been suggested (*17*).

Past work has often struggled to fit dinosaurs into a simple energetic dichotomy; our work suggests that an intermediate view (*17*, *21*) is more likely. Although dinosaur growth rates vary, they cluster most closely to those of thermally intermediate taxa (Figs. 1 and 2), which we term mesotherms. Mesothermic tuna, lamnid sharks, and the leatherback turtle rely on metabolic heat to raise their body temperature (T_b) above the ambient temperature (T_a) but do not metabolically defend a thermal set point as endotherms do (*16*, *22*). This reliance on metabolic heat distinguishes them from other large homeothermic reptiles, such as crocodiles (*23*), which bask to elevate T_b. The echidna, while maintaining a set point of ~31°C, shows remarkable lability, because T_b values can range over 10°C while it is active (*24*). Unlike hibernating mammals or torpid hummingbirds, this variability is externally imposed. Collectively, these animals are distinguished from endotherms and ectotherms by a weak or absent metabolic defense of a thermal set point but sufficient internal heat production to maintain $T_b > T_a$ when T_a is low [see (*9*) for further discussion]. Although some feathered dinosaurs may have been endotherms, they would have been uniquely low-powered compared to extant birds and mammals. We suggest that mesothermy may have been common among dinosaurs, ranging from modest metabolic control of T_b, as seen in furred echidnas, to the absent metabolic defense observed in tuna and leatherback turtles. Analysis of fossil isotopes, which can shed light on body temperatures, will be useful in testing this hypothesis. In particular, attention to neonate and juvenile dinosaurs in seasonally cool environments, such as polar regions, may help distinguish among thermoregulatory states.

Dinosaurs dominated the flux of matter and energy in terrestrial ecosystems for more than 135 million years. Consequently, our results have important implications for understanding ancient Mesozoic ecosystems. We emphasize the primary importance of comparative energetics for integrating form, function, and diversity. Knowing only two facts from the fossil record—adult mass and maximum growth rate—we show that the metabolic rates of extinct clades can be predicted with accuracy. Such an approach will be useful in resolving the energetics of metabolically ambiguous taxa, such as pterosaurs, therapsids, and Mesozoic birds.

REFERENCES AND NOTES

1. K. Padian, A. J. de Ricqlès, J. R. Horner, *Nature* **412**, 405–408 (2001).
2. P. M. Sander *et al.*, *Biol. Rev. Camb. Philos. Soc.* **86**, 117–155 (2011).
3. R. A. Eagle *et al.*, *Science* **333**, 443–445 (2011).
4. J. H. Brown, J. F. Gillooly, A. P. Allen, V. M. Savage, G. B. West, *Ecology* **85**, 1771–1789 (2004).
5. P. Else, A. Hulbert, *Am. J. Physiol. Regul. Integr. Comp. Physiol.* **240**, R3–R9 (1981).
6. J. F. Gillooly, J. H. Brown, G. B. West, V. M. Savage, E. L. Charnov, *Science* **293**, 2248–2251 (2001).
7. G. M. Erickson, K. C. Rogers, S. A. Yerby, *Nature* **412**, 429–433 (2001).
8. A. H. Lee, S. Werning, *Proc. Natl. Acad. Sci. U.S.A.* **105**, 582–587 (2008).
9. See the supplementary materials.
10. F. Seebacher, *Paleobiology* **29**, 105–122 (2003).
11. R. H. Peters, *The Ecological Implications of Body Size* (Cambridge Univ. Press, Cambridge, MA, 1983).
12. C. R. White, N. F. Phillips, R. S. Seymour, *Biol. Lett.* **2**, 125–127 (2006).
13. T. J. Case, *Q. Rev. Biol.* **53**, 243–282 (1978).
14. G. B. West, J. H. Brown, B. J. Enquist, *Nature* **413**, 628–631 (2001).
15. C. Hou *et al.*, *Science* **322**, 736–739 (2008).
16. D. Bernal, K. A. Dickson, R. E. Shadwick, J. B. Graham, *Comp. Biochem. Physiol. A Mol. Integr. Physiol.* **129**, 695–726 (2001).
17. G. M. Erickson *et al.*, *PLOS ONE* **4**, e7390 (2009).
18. A. Chinsamy, *Mesozoic Birds: Above the Heads of Dinosaurs* (Univ. of California Press, Berkeley, CA, 2002), pp. 421–431.

Downloaded from http://science.sciencemag.org/ on July 5, 2016

19. E. L. Charnov, D. Berrigan, *Evol. Anthropol.* **1**, 191–194 (1993).
20. K. Isler, C. P. van Schaik, *J. Hum. Evol.* **57**, 392–400 (2009).
21. R. Reid, in *The Complete Dinosaur*, M. K. Brett-Surman, T. R. Holtz, J. O. Farlow, Eds. (Indiana Univ. Press, Bloomington, IN, 2012), pp. 873–24.
22. F. V. Paladino, M. P. O'Connor, J. R. Spotila, *Nature* **344**, 858–860 (1990).
23. F. Seebacher, G. C. Grigg, L. A. Beard, *J. Exp. Biol.* **202**, 77–86 (1999).
24. P. Brice, G. C. Grigg, L. A. Beard, J. A. Donovan, *Aust. J. Zool.* **50**, 461–475 (2002).

ACKNOWLEDGMENTS

This work was supported by a fellowship from the Program in Interdisciplinary Biological and Biomedical Sciences at the University of New Mexico (grant no. T32EB009414 from the National Institute of Biomedical Imaging and Bioengineering to F.A.S. and J. H. Brown). B.J.E. was supported by an NSF CAREER and ATB Award (EF 0742800). We thank C. White and two anonymous reviewers for valuable feedback on our manuscript and N. Milan for assistance with the figures. Data are available in the supplementary materials.

SUPPLEMENTARY MATERIALS

www.sciencemag.org/content/344/6189/1268/suppl/DC1
Figs. S1 to S15
Tables S1 to S4
References (*25*–*396*)

10 March 2014; accepted 8 May 2014
10.1126/science.1253143

NONHUMAN GENETICS

Strong male bias drives germline mutation in chimpanzees

Oliver Venn,[1] Isaac Turner,[1] Iain Mathieson,[1]* Natasja de Groot,[2] Ronald Bontrop,[2] Gil McVean[1]†

Germline mutation determines rates of molecular evolution, genetic diversity, and fitness load. In humans, the average point mutation rate is 1.2×10^{-8} per base pair per generation, with every additional year of father's age contributing two mutations across the genome and males contributing three to four times as many mutations as females. To assess whether such patterns are shared with our closest living relatives, we sequenced the genomes of a nine-member pedigree of Western chimpanzees, *Pan troglodytes verus*. Our results indicate a mutation rate of 1.2×10^{-8} per base pair per generation, but a male contribution seven to eight times that of females and a paternal age effect of three mutations per year of father's age. Thus, mutation rates and patterns differ between closely related species.

Accurate determination of the rate of de novo mutation in the germ line of a species is central to the dating of evolutionary events. However, because mutations are rare events, efforts to measure the rate in humans have typically been indirect, calculated from the incidence of genetic disease or sequence divergence (*1*–*4*). However, high-throughput sequencing technologies have enabled direct estimates of the mutation rate from comparison of the genome sequence of family members (*5*–*8*). Unexpectedly, these studies have indicated a mutation rate of, on average, ~1.2×10^{-8} per base pair per generation, or ~0.5×10^{-9} per base pair per year, approximately half that inferred from phylogenetic approaches (*1*, *9*). Moreover, they have demonstrated a substantial male bias to mutation, such that three to four times as many autosomal mutations occur in the male compared to the female germ line (*6*, *7*). Male bias is largely caused by an increase in the rate of paternal but not maternal mutation with the age of the parent; approximately two additional mutations per year of father's age at conception (*7*). This difference is consistent with ongoing cell division in the male germ line but not in females (*10*).

An alternative approach for estimating the extent of male bias is to compare rates of sequence divergence on the autosomes (which spend equal time in the male and female germ lines) and the X chromosome (which spends two-thirds of the time in females) (*2*, *11*). Such indirect approaches broadly agree with direct estimates in humans, but suggest that male bias may be stronger in chimpanzees (*12*). To test this hypothesis, we sequenced the genomes of nine members of a three-generation pedigree of Western chimpanzees, *Pan troglodytes verus* (Fig. 1A and fig. S1). One trio was sequenced at high depth (average 51×), while other family members were sequenced to an average of 27× (table S1). We inferred the structure of recombination and transmission across the pedigree (Fig. 1B), which enabled us to detect de novo point mutations in regions of high sequence complexity and to remove artifacts caused by mismapping, sequence that is absent from the reference genome, and reference misassembly (*13*).

We used a probabilistic approach that, at a given site, compared the likelihood of different models for genetic variation inconsistent with the inferred transmission: genotyping error at a segregating variant, de novo mutation, single-gene conversion event, segregating deletion and erroneous call (Fig. 1C). The design was expected to enable haplotype phasing through transmission for 99.2% of sites that were heterozygous in the founders and 87.5% of de novo mutation events inherited by chimpanzee F (Fig. 1A). Read-based phasing was used to phase de novo events in other offspring, and we performed independent validation to assess the accuracy of de novo variant calls. The false-negative rate was estimated from allele-dropping simulations (*13*).

Across the genomes of the nine pedigree members, we called 4.1 million variants [single-nucleotide polymorphisms (SNPs) and short insertions and deletions (indels)] using a mapping-based approach and 3.0 million variants using an assembly-based approach (*14*). Genotype data confirmed expected pedigree relationships (fig. S2). The intersection of call sets (1.6 million sites with a transition-transversion ratio of 2.2) established the underlying structure of recombination and transmission across the pedigree with a robust version of the Lander-Green algorithm (fig. S3). Briefly, this is a two-stage strategy of identifying dominant inheritance vectors over 1-Mb intervals, followed by fine-mapping of cross-over breakpoints, which guards against problems caused by false-positive variants and genotyping errors (*13*). Across the pedigree, we identified 375 cross-over events, with a distribution similar to that of human homologs, with the exception of human chromosome 2, which is a fusion of the chimpanzee chromosomes 2A and 2B (*15*) (Fig. 2A, fig. S4, and tables S2 and S3).

Overall, we estimate the sex-averaged autosomal genetic map length to be 3150 cM [95% equal-tailed probability interval (ETPI) 2850 to 3490], compared to 3505 cM in humans (*16*, *17*). On the X chromosome, we detected nine cross-over events in the non-pseudoautosomal (non-PAR) region, indicating a female-specific genetic map length of 160 cM (95% ETPI 83 to 300), compared to 180 cM in humans. On the pseudoautosomal region (PAR), we detected four male cross-overs, giving a male-specific estimate of 34 cM (95% ETPI 28 to 180; tables S4 and S5), in agreement with estimates in humans (*13*). Males have 58% of the autosomal cross-over events of females and, unlike females, show an increase in cross-over frequency toward the telomere (Fig. 2B), similar to humans (fig. S5). We also observed a decrease in cross-over frequency with maternal (2.65 cM per year, linear model $P = 0.025$), but not paternal age (Fig. 2C). However, this observation could be explained by between-female variation (linear model $P = 0.13$, allowing for a maternal effect). The median interval size to which cross-over events can be localized is 7.0 kb, with 95% of all intervals localized to within 80 kb (excluding complex cross-over events), with cross-over events enriched in regions inferred to have

[1]Wellcome Trust Centre for Human Genetics, Roosevelt Drive, Oxford, OX3 7BN, UK. [2]Biomedical Primate Research Centre, Lange Kleiweg 161, 2288 GJ Rijswijk, Netherlands. *Present address: Department of Genetics, Harvard Medical School, 77 Avenue Louis Pasteur, Boston, MA 02115 USA. †Corresponding author. E-mail: mcvean@well.ox.ac.uk

Downloaded from http://science.sciencemag.org/ on July 5, 2016

Science
AAAS

Evidence for mesothermy in dinosaurs
John M. Grady, Brian J. Enquist, Eva Dettweiler-Robinson, Natalie A. Wright and Felisa A. Smith (June 12, 2014)
Science **344** (6189), 1268-1272. [doi: 10.1126/science.1253143]

Editor's Summary

Not too fast, not too slow, somewhere in between

In early depictions, dinosaurs lumbered slowly, dragging their tails. More recently, we have imagined them lifting their tails and running. The question boils down to whether dinosaurs had energetic systems closer to those of rapidly metabolizing mammals and birds, or to those of slower reptiles that do not internally regulate their body temperature. However, determining the metabolic rate of extinct organisms is no easy task. Grady *et al.* analyzed a huge data set on growth rate in both extinct and living species, using a method that considers body temperature and body size. Dinosaur metabolism seems to have been neither fast nor slow, but somewhere in the middle ––so, dinosaurs did not fully regulate their internal temperature but they were also not entirely at the whim of the environment; neither slow goliaths nor supercharged reptiles.

Science, this issue p. 1268

This copy is for your personal, non-commercial use only.

Article Tools Visit the online version of this article to access the personalization and article tools:
http://science.sciencemag.org/content/344/6189/1268

Permissions Obtain information about reproducing this article:
http://www.sciencemag.org/about/permissions.dtl

Science (print ISSN 0036-8075; online ISSN 1095-9203) is published weekly, except the last week in December, by the American Association for the Advancement of Science, 1200 New York Avenue NW, Washington, DC 20005. Copyright 2016 by the American Association for the Advancement of Science; all rights reserved. The title *Science* is a registered trademark of AAAS.

Downloaded from http://science.sciencemag.org/ on July 5, 2016